Problem Chosen	2026 MCM/ICM Summary Sheet	Team Control Number
A		2631793

Problem. Build a continuous-time model for a smartphone Li-ion battery that predicts remaining time-to-empty under varying usage and ambient conditions.
Model. We propose a **continuous electro-thermal SOC ODE model** coupling interpretable power decomposition, lumped thermal dynamics, and temperature-dependent effective capacity.
Algorithm. Using a **numerical ODE integration + event stopping algorithm**, we compute time-to-empty and generate SOC/temperature/power traces for attribution.
Results. The **power–thermal–SOC framework** predicts 8.785 h (light, room), 3.208 h (gaming, room), and 3.286 h (navigation, cold); sensitivity ranks SOH first ($S = 1.194$), and Monte Carlo yields [2.762, 3.680] h (95%) for gaming.

Table 1: Key outcomes (used in the report).

Scenario	T_{empty} (h)	$\overline{P}_{\text{tot}}$ (W)	$\overline{f_T}$
LightUse_RoomTemp	8.785	1.652	1.000
HeavyUse_Gaming_RoomTemp	3.208	4.525	1.000
Navigation_ColdOutdoor	3.286	3.957	0.893

Key takeaways.

- **Power-dominant vs. capacity-dominant:** gaming shortens life mainly via higher mean power; cold navigation shortens life mainly via reduced usable capacity.
- **Most influential parameter:** SOH dominates time-to-empty ($S = 1.194$), implying that battery health can be the primary constraint.
- **Uncertainty is non-trivial:** stochastic background/network loads can shift lifetime by tens of minutes, motivating interval predictions.

Abstract

Smartphone battery life varies substantially from day to day because energy drain depends on (i) time-varying component loads (screen, CPU, network, GPS, and background tasks) and (ii) temperature-dependent electrochemical behavior that changes the usable capacity of a Li-ion cell. To meet the requirement of a continuous-time model that returns $SOC(t)$ and predicts time-to-empty under realistic conditions, we develop a mechanistic yet interpretable electro-thermal modeling framework.

Our approach decomposes total power into a baseline plus usage-driven modules, $P_{\mathrm{tot}}(t) = P_0 + P_{\mathrm{scr}}(t) + P_{\mathrm{cpu}}(t) + P_{\mathrm{net}} + P_{\mathrm{gps}}(t) + P_{\mathrm{bg}}$, where screen and CPU powers scale nonlinearly with normalized brightness $b(t)$ and effective CPU utilization $u_{\mathrm{eff}}(t)$. This demand drives both the charge depletion process and the thermal state of the battery. We couple power demand to a lumped thermal balance, $C_{\mathrm{th}}\frac{\mathrm{d}T(t)}{\mathrm{d}t} = h(T_{\mathrm{amb}} - T(t)) + \eta P_{\mathrm{tot}}(t)$, in which a fraction of electrical power becomes heat and the device exchanges heat with ambient temperature T_{amb}. Temperature feeds back through a bounded temperature-capacity factor $f_T(T)$ that modifies the effective usable charge reservoir, $Q_{\mathrm{eff}}(t) = 3600 Q_{\mathrm{nom}} SOH\, f_T(T(t))$, where SOH captures battery health. Finally, SOC evolves as a continuous-time energy-based ODE, $\frac{\mathrm{d}SOC(t)}{\mathrm{d}t} = -\frac{P_{\mathrm{tot}}(t)}{V(SOC(t))Q_{\mathrm{eff}}(t)}$, and time-to-empty is computed by event stopping at a practical cutoff SOC_{min}.

This structure is continuous-time, physically consistent (energy/heat balances), and modular: additional app loads or sensors can be incorporated by extending $P_{\mathrm{tot}}(t)$ without altering the ODE core. Using three representative scenarios, the model predicts $T_{\mathrm{empty}} = 8.785$ h for light use at room temperature, 3.208 h for heavy gaming at room temperature, and 3.286 h for navigation in cold ambient conditions. These results reveal two distinct mechanisms of reduced lifetime: gaming is power-dominated (mean power rises to 4.525 W), while cold navigation is capacity-dominated (mean power is lower at 3.957 W, yet $\overline{f_T} = 0.893$ reduces usable charge). A one-at-a-time sensitivity analysis ranks SOH as the most influential driver ($S = 1.194$), followed by network and display parameters, while thermal parameters have negligible influence under room-temperature conditions because the temperature remains far from throttling thresholds. Monte Carlo simulations capture uncertainty from stochastic background/network loads and yield a 95% interval of [2.762, 3.680] h for the gaming scenario, indicating that user-facing predictions should be communicated with uncertainty bands rather than a single point estimate. Overall, the framework provides a quantitative and interpretable foundation for diagnosing battery drain and producing actionable strategies (brightness reduction, load management, network optimization, and cold mitigation) tailored to whether the dominant limitation is power draw or usable capacity.

Contents

Executive Overview

We build a continuous-time electro-thermal model that links usage to energy drain through an interpretable power decomposition, and links environment to discharge through a temperature-dependent effective capacity. The model outputs the full trajectories $SOC(t)$ and $T(t)$, identifies time-to-empty via an event condition, and supports sensitivity and uncertainty analysis.

Table 2: Key numerical outcomes used throughout the report.

Scenario	T_{empty} (h)	$\overline{P}_{\text{tot}}$ (W)	$\overline{f_T}$
LightUse_RoomTemp	8.785	1.652	1.000
HeavyUse_Gaming_RoomTemp	3.208	4.525	1.000
Navigation_ColdOutdoor	3.286	3.957	0.893

High-level conclusions.

- **Mechanism separation:** gaming shortens life mainly via higher mean power; cold navigation shortens life via reduced usable capacity.
- **Dominant driver:** sensitivity ranks SOH first; therefore aging/health often dominates over short-term usage tweaks.
- **Risk-aware prediction:** Monte Carlo intervals quantify realistic variability caused by background/network fluctuations.

1 Restatement of the Problem (in our own words)

A smartphone's remaining battery life depends on how quickly stored energy is consumed, which varies with user behavior (screen brightness, compute load, network activity, GPS usage, and background tasks) and with environmental conditions (ambient temperature). We must develop a *continuous-time* mathematical model that returns $SOC(t)$ and predicts remaining time-to-empty under different scenarios. We also evaluate the model through reasonableness checks, quantify sensitivity to key parameters, quantify uncertainty, and translate findings into practical recommendations.

2 Assumptions

We adopt four assumptions to ensure interpretability and identifiability while capturing the dominant physics.

A1: Energy-dominant discharge: over a single discharge run, self-discharge and calendar aging are negligible; energy is consumed only by device power demand.

A2: Additive module power: total demand is the sum of module powers (screen/CPU/network/GPS/background) and a baseline, enabling power attribution.

A3: Lumped thermal state: battery temperature can be represented by a single state $T(t)$ with linear heat exchange to ambient.

A4: Temperature affects usable capacity: temperature influences discharge primarily through a capacity factor $f_T(T)$ that modifies effective usable charge.

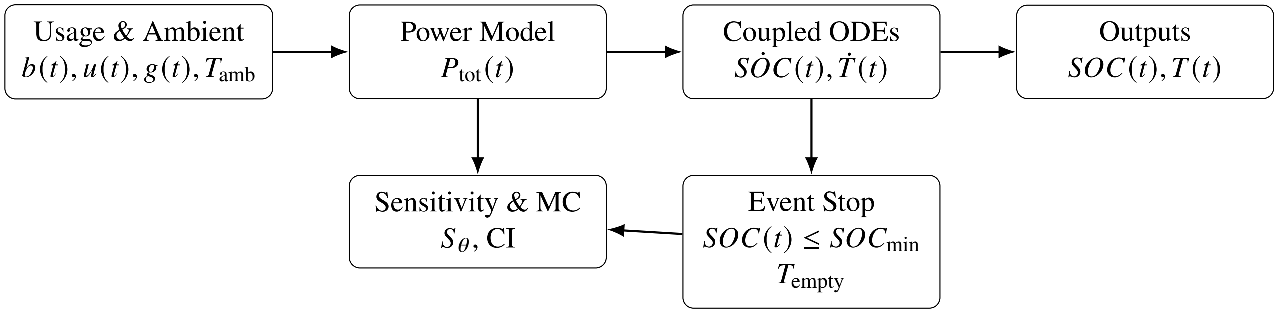

Figure 1: Flowchart of the electro-thermal modeling framework.

Usage and ambient inputs determine total power, which drives coupled continuous-time SOC and thermal dynamics. Time-to-empty is computed by event stopping, and sensitivity/Monte Carlo quantify robustness.

3 Problem Analysis and Modeling Roadmap

Battery drain is fundamentally driven by power demand. However, temperature can change usable capacity and can trigger throttling that changes demand. Therefore, a realistic model must (i) map usage signals to $P_{tot}(t)$, (ii) propagate heat to obtain $T(t)$, and (iii) propagate charge to obtain $SOC(t)$ and time-to-empty. We also include sensitivity and uncertainty modules so the framework can identify influential drivers and quantify robustness.

4 Notation

Table 3: Key symbols used in the model.

Symbol	Meaning	Unit
t	time	s
$SOC(t)$	state of charge	–
$T(t)$	battery temperature	°C
T_{amb}	ambient temperature	°C
$P_{\text{tot}}(t)$	total power demand	W
Q_{nom}	nominal battery capacity	Ah
SOH	state of health	–
$f_T(T)$	temperature capacity factor	–
C_{th}	thermal capacitance	J/°C
h	heat transfer coefficient	W/°C
η	heat conversion fraction	–
T_{empty}	time-to-empty	h

5 Model Development

5.1 Design Philosophy

The model must satisfy three constraints simultaneously: (i) *continuous time* (explicit ODEs), (ii) *physical interpretability* (clear mapping from usage to drain), and (iii) *extensibility* (new apps/sensors can be incorporated). We thus build a coupled electro-thermal system consisting of an additive power module, a lumped thermal ODE, and an SOC ODE with temperature-modulated usable charge.

5.2 Power Decomposition: from usage to demand

Idea. Battery drain is ultimately caused by power demand. Since screen, CPU, radios, and sensors draw power in parallel, the simplest interpretable structure is an additive decomposition. This choice also enables direct attribution: reducing a module's coefficient increases predicted time-to-empty in a transparent manner.

$$P_{\text{tot}}(t) = P_0 + P_{\text{scr}}(t) + P_{\text{cpu}}(t) + P_{\text{net}} + P_{\text{gps}}(t) + P_{\text{bg}}. \tag{1}$$

Screen module. Display/backlight power increases nonlinearly with brightness:

$$P_{\text{scr}}(t) = \alpha_{\text{scr}} + \beta_{\text{scr}}\, b(t)^{\gamma_{\text{scr}}}, \quad b(t) \in [0,1]. \tag{2}$$

CPU module. CPU power is convex in utilization/frequency (dynamic power $\propto fV^2$). We use:

$$P_{\text{cpu}}(t) = \alpha_{\text{cpu}} + \beta_{\text{cpu}}\, u_{\text{eff}}(t)^{\gamma_{\text{cpu}}}, \quad u_{\text{eff}}(t) \in [0,1]. \tag{3}$$

GPS module. GPS is frequently on/off:

$$P_{\text{gps}}(t) = p_{\text{gps}}\, g(t), \quad g(t) \in \{0,1\}. \tag{4}$$

Here P_{net} and P_{bg} summarize network overhead and background activity. In uncertainty analysis we treat them as stochastic drivers to reflect real-world variability.

5.3 Thermal Model: heat balance and interpretability

Idea. Temperature affects usable capacity and can trigger throttling. A full spatial thermal PDE is unnecessary in contest settings; a lumped temperature state captures first-order effects while keeping parameters identifiable.

$$C_{\mathrm{th}} \frac{\mathrm{d}T(t)}{\mathrm{d}t} = h\,(T_{\mathrm{amb}} - T(t)) + \eta\, P_{\mathrm{tot}}(t). \tag{5}$$

5.4 Thermal Throttling: closing the feedback loop

Idea. Smartphones throttle CPU when temperature is high. Including throttling prevents unphysical overheating under heavy loads and preserves realism in stress scenarios.

$$u_{\max}(T) = \begin{cases} 1, & T \le T_{\mathrm{th}}, \\ \max(u_{\min},\ 1 - \rho\,(T - T_{\mathrm{th}}))\,, & T > T_{\mathrm{th}}, \end{cases} \tag{6}$$

$$u_{\mathrm{eff}}(t) = \min(u(t), u_{\max}(T(t)))\,. \tag{7}$$

5.5 Temperature-Dependent Effective Capacity

Idea. Low temperature reduces reaction kinetics and increases internal resistance, so a phone reaches cutoff sooner for the same nominal charge. We capture this by a bounded temperature factor $f_T(T)$ and battery health SOH:

$$Q_{\mathrm{eff}}(t) = 3600\, Q_{\mathrm{nom}}\, SOH\, f_T(T(t))\,. \tag{8}$$

$$f_T(T) = \begin{cases} \max(f_{\min},\ 1 - \kappa_c(T_c - T))\,, & T < T_c, \\ 1, & T_c \le T \le T_h, \\ \max(f_{\min},\ 1 - \kappa_h(T - T_h))\,, & T > T_h. \end{cases} \tag{9}$$

5.6 SOC Dynamics and Time-to-Empty

Idea. SOC should decrease faster when power is higher or usable capacity is lower. Since $P = VI$, we infer $I(t) = P_{\mathrm{tot}}(t)/V(SOC)$ and divide by usable charge.

We use a simple bounded SOC-voltage map:

$$V(SOC) = \max(V_{\min},\ v_0 + v_1\, SOC)\,. \tag{10}$$

Then:

$$\frac{\mathrm{d}SOC(t)}{\mathrm{d}t} = -\frac{P_{\mathrm{tot}}(t)}{V(SOC(t))\ Q_{\mathrm{eff}}(t)}. \tag{11}$$

Practical “empty” occurs at a cutoff rather than $SOC = 0$, so we define:

$$T_{\mathrm{empty}} = \inf\{t > 0 :\ SOC(t) \le SOC_{\min}\}\,. \tag{12}$$

6 Parameterization and Calibration

6.1 Parameter tiers and identifiability

To keep the model reproducible yet realistic, we assign parameters in three tiers:

- **Physics-scale parameters** (voltage window, thermal time constant) chosen from standard battery and heat-transfer references.

Table 4: Representative parameter values used in simulations.

Category	Parameter	Value	Unit
Battery	Q_{nom}	5.0	Ah
Battery	SOH	1.0	–
Cutoff	SOC_{min}	0.05	–
Voltage	V_{min}	3.3	V
Voltage	v_0, v_1	3.3, 0.9	V
Thermal	C_{th}	1200	J/°C
Thermal	h	1.8	W/°C
Thermal	η	0.15	–
Throttle	T_{th}	45	°C
Throttle	u_{min}, ρ	0.60, 0.03	–, 1/°C
Cap.-temp	T_c, T_h	10, 40	°C
Cap.-temp	κ_c, κ_h	0.005, 0.003	1/°C
Cap.-temp	f_{min}	0.70	–

- **Scenario inputs** ($b(t)$, $u(t)$, $g(t)$, T_{amb}) to represent typical usage patterns.
- **Lumped demand coefficients** (P_0, P_{net}, P_{bg}, screen/CPU coefficients) set so mean powers match realistic drain regimes (light use: 1–2 W; gaming: 4–6 W; navigation: 3–5 W).

This tiering avoids over-parameterization that cannot be justified without proprietary telemetry.

6.2 Representative parameter set

6.3 Calibration logic (contest-appropriate)

We calibrate lumped demand coefficients to match order-of-magnitude expectations for smartphone power regimes. We then verify directionality: increasing brightness, CPU utilization, and network power decreases time-to-empty; warming ambient increases time-to-empty in cold scenarios through higher $f_T(T)$.

7 Sanity Checks and Qualitative Validation

7.1 Dimensional consistency

Equation (11) has units of 1/s because P is J/s and VQ_{eff} is J. Equation (5) is consistent because both sides have units of power (J/s).

7.2 Monotonicity tests

The model preserves expected monotonicity:

- Increasing $P_{\text{tot}}(t)$ increases $\left|\frac{\mathrm{d}SOC}{\mathrm{d}t}\right|$ and reduces T_{empty} (Eq. (11)).
- Lowering $T(t)$ in cold regimes reduces $f_T(T)$, reduces $Q_{\text{eff}}(t)$, and reduces T_{empty} (Eqs. (8)–(11)).
- Improving SOH increases $Q_{\text{eff}}(t)$ approximately linearly and increases T_{empty} (Eq. (8)).

7.3 Extreme-case behavior

If $h \to \infty$, then $T(t) \to T_{\text{amb}}$ and the model reduces to an electro-only SOC ODE with temperature-fixed capacity. If $\eta \to 0$, self-heating vanishes and $T(t)$ relaxes toward ambient. These limits are physically meaningful.

8 Results

8.1 Scenario-Level Comparison

Table 5 summarizes time-to-empty, average power, peak power, and thermal/capacity indicators. Two distinct mechanisms emerge.

Power-dominant drain (gaming). Mean power increases from 1.652 W (light use) to 4.525 W (gaming), a 2.74× increase, reducing lifetime from 8.785 h to 3.208 h (a 63.5% reduction). This shows that heavy interactive workloads primarily shorten battery life by elevating sustained demand.

Capacity-dominant drain (cold navigation). In cold navigation, mean power (3.957 W) is lower than gaming, yet lifetime is comparable (3.286 h). The key difference is $\overline{f_T} = 0.893$, which reduces usable charge in Eq. (8). Thus, cold conditions can erase the advantage of lower power by lowering effective capacity.

Table 5: Scenario-level quantitative results (from simulation outputs).

Scenario	T_{empty} (h)	$\overline{P}_{\text{tot}}$ (W)	$P_{\max}$ (W)	$T_{\max}$ (°C)	$\overline{f_T}$
LightUse_RoomTemp	8.785	1.652	1.877	25.626	1.000
HeavyUse_Gaming_RoomTemp	3.208	4.525	5.726	26.909	1.000
Navigation_ColdOutdoor	3.286	3.957	4.288	1.429	0.893

How to read Figure 2. Time-to-empty is computed as the first-hitting time of $SOC(t) \le SOC_{\min}$ (Eq. (12)). Therefore, differences in T_{empty} reflect differences in the *average depletion rate* $|\mathrm{d}SOC/\mathrm{d}t|$ (Eq. (11)), which is governed by (i) mean demand $\overline{P}_{\text{tot}}$ and (ii) usable charge $Q_{\text{eff}} = 3600 Q_{\text{nom}} SOH\, f_T(T)$ (Eq. (8)).

Quantitative comparison. Light use lasts 8.785 h, while gaming and cold navigation last 3.208 h and 3.286 h, respectively. Gaming is shorter mainly because $\overline{P}_{\text{tot}}$ increases from 1.652 W to 4.525 W (2.74×), whereas cold navigation has lower mean power (3.957 W) but reduced capacity $\overline{f_T} = 0.893$. Thus, two scenarios can yield similar lifetimes (≈ 3.2 h) for different reasons.

Mechanism takeaway. Because the limiting mechanism differs, effective interventions differ: for gaming, reduce workload/brightness/network overhead; for cold navigation, increase temperature (insulation, keeping the phone warm) to raise $f_T(T)$ and thus Q_{eff}.

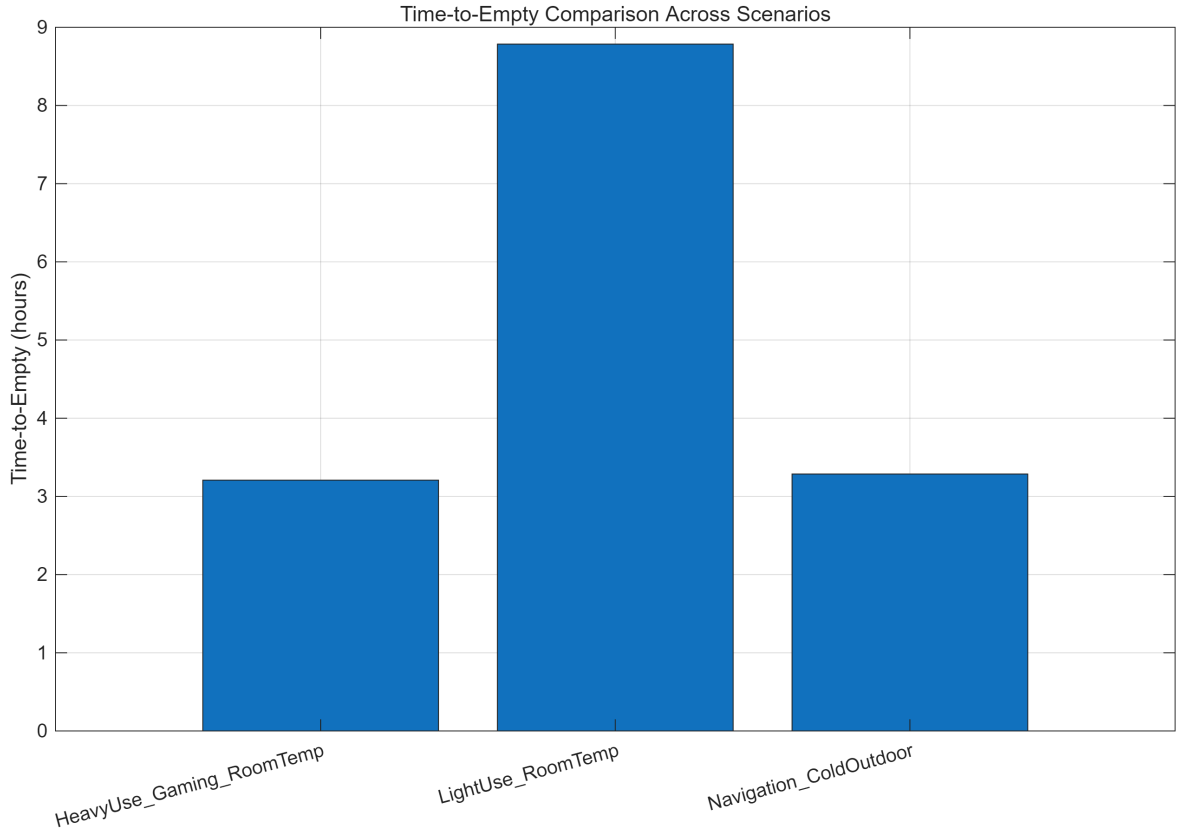

Figure 2: Predicted time-to-empty T_{empty} across scenarios.

Gaming is power-dominant (high $\overline{P}_{\text{tot}}$), while cold navigation is capacity-dominant (low $\overline{f_T}$).

8.2 Trajectory Evidence: SOC and Temperature

Figures 3–5 provide time-domain evidence supporting the mechanism separation above. Each plot jointly displays $SOC(t)$ and $T(t)$, allowing us to distinguish whether lifetime is controlled mainly by demand (P_{tot}) or by supply (Q_{eff} via f_T).

Figure 3 (Light use, room). The SOC curve is close to linear over most of the horizon, indicating that $P_{\text{tot}}(t)$ is nearly constant (Eq. (1)). In this regime, Eq. (11) behaves approximately as a constant-slope depletion model, so lifetime is mainly controlled by the mean power level rather than transients. The temperature trajectory quickly approaches a narrow band around ambient ($\approx 25°$C), implying that $\eta P_{\text{tot}}(t)$ is small and the thermal state is dominated by heat exchange $h(T_{\text{amb}} - T)$ (Eq. (5)). Consequently $f_T(T) \approx 1$ and throttling is inactive.

Interpretation. This scenario serves as a baseline demonstrating power-driven discharge: when temperature stays in the comfortable range, variations in T_{empty} are mainly explained by differences in $\overline{P}_{\text{tot}}$.

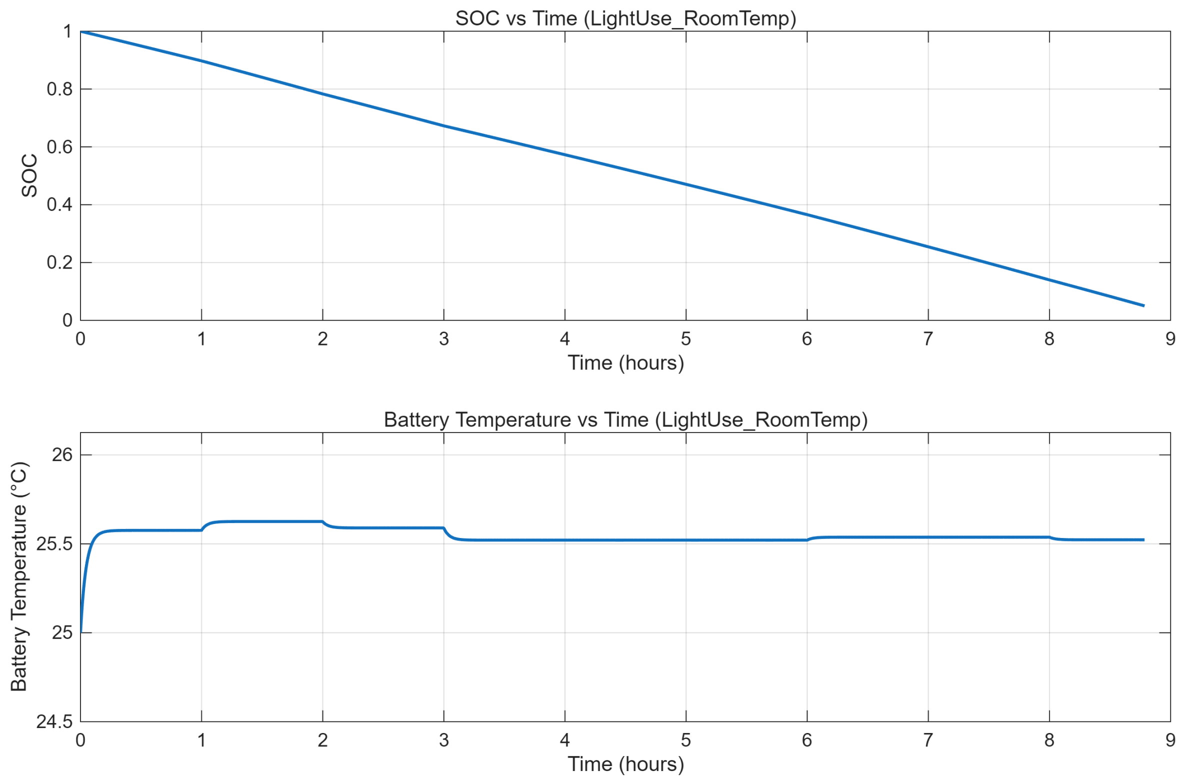

Figure 3: SOC and temperature trajectories for `LightUse_RoomTemp`.

Nearly constant demand produces a near-linear SOC decline; temperature stays near ambient so $f_T(T) \approx 1$ and throttling remains inactive.

Figure 4 (Gaming, room). Compared to light use, SOC declines much faster, consistent with the higher mean power ($\overline{P}_{\text{tot}} = 4.525$ W). Mild changes in slope correspond to changes in module demand (e.g., gaming bursts vs. steadier periods). Temperature rises to a modest plateau ($T_{\max} \approx 26.9$°C), indicating self-heating exists but is limited by ambient exchange in Eq. (5). Because $T(t)$ remains far below the throttling threshold $T_{\text{th}} = 45$°C (Table 4), the effective utilization $u_{\text{eff}}(t) = \min(u(t), u_{\max}(T(t)))$ (Eq. (7)) essentially equals $u(t)$. Therefore, the lifetime reduction here is *not* throttle-dominant; it is power-dominant.

Interpretation. This plot anticipates the sensitivity results: parameters increasing mean demand (network, screen scaling, CPU scaling) strongly affect T_{empty}, while thermal parameters remain weak at room temperature because $T(t)$ never approaches T_{th}.

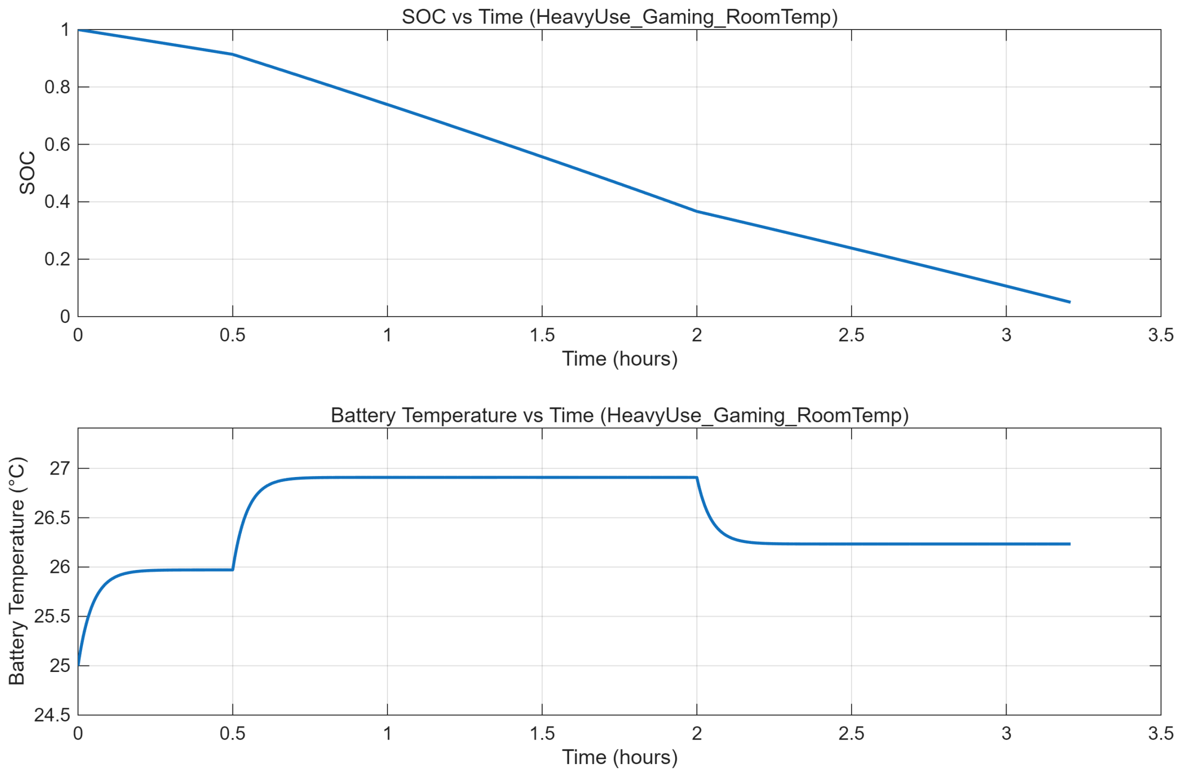

Figure 4: SOC and temperature trajectories for `HeavyUse_Gaming_RoomTemp`.

SOC drops steeply due to sustained high demand; temperature rises modestly and remains below throttling, so the lifetime loss is power-dominant rather than throttle-dominant.

Figure 5 (Navigation, cold). In cold ambient conditions, $T(t)$ stays near 0–2°C, placing the battery in the low-temperature branch of $f_T(T)$ (Eq. (9)). As a result, usable capacity decreases: $\overline{f_T} = 0.893$ (Table 5). Even though mean power ($\overline{P}_{\text{tot}} = 3.957$ W) is lower than gaming, the reduced Q_{eff} increases the depletion rate in Eq. (11), yielding a similar time-to-empty (3.286 h). This demonstrates a *capacity-dominant* limitation: improving thermal conditions can extend lifetime even if usage power remains unchanged.
Interpretation. Unlike gaming, the most effective intervention here is increasing $T(t)$ (e.g., insulation, keeping the device warm) to raise $f_T(T)$ and thus Q_{eff}.

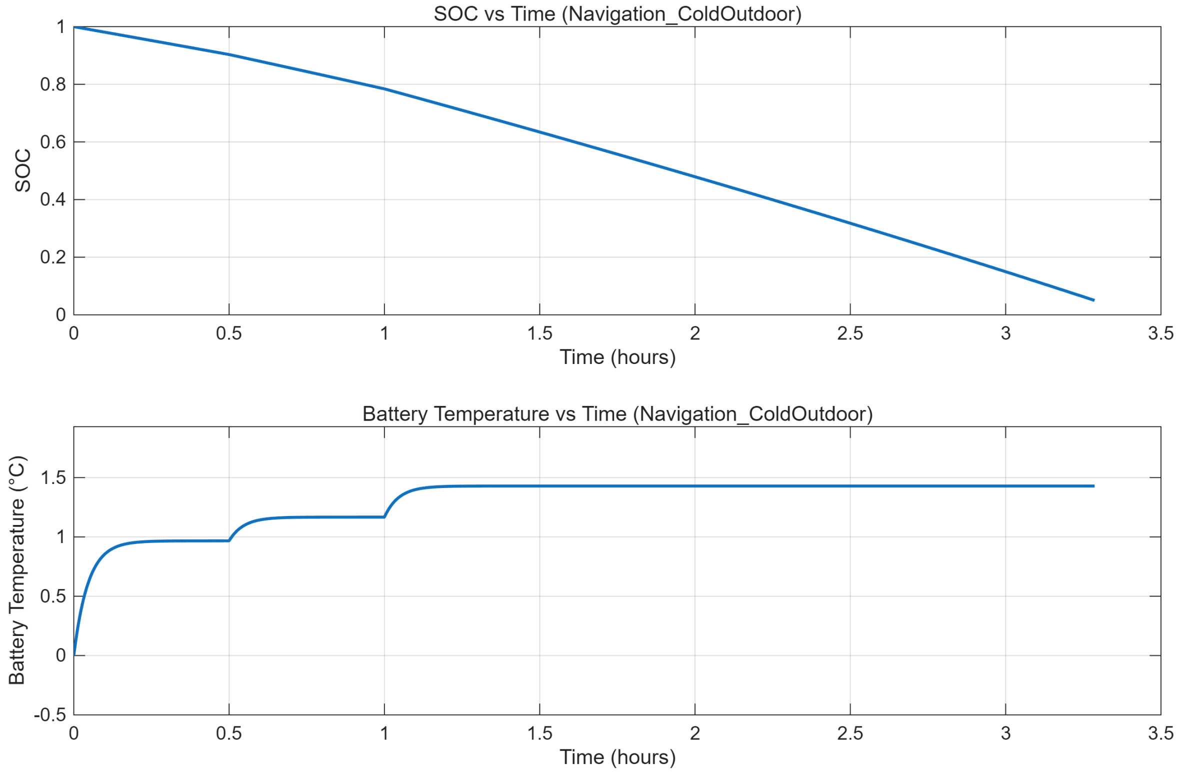

Figure 5: SOC and temperature trajectories for `Navigation_ColdOutdoor`.

Cold ambient keeps $T(t)$ low, pushing $f_T(T) < 1$ and shortening lifetime mainly through reduced effective capacity $Q_{\mathrm{eff}}(t)$.

8.3 Power Attribution: Why gaming drains quickly

Figure 6 (Gaming power). The top panel shows a step-like increase in $P_{\mathrm{tot}}(t)$ during intensive gaming periods, followed by a lower plateau when workload relaxes. This explains the piecewise SOC slope in Figure 4. The stacked breakdown indicates that CPU and network account for most of the incremental demand above baseline, while screen remains a persistent contributor. When $f_T(T) \approx 1$ (room temperature), time-to-empty is approximately inversely proportional to mean demand, so sustained increases in CPU/network power translate into large lifetime reductions.

Actionable link. This attribution supports targeted recommendations: lowering graphics/CPU intensity and improving signal quality (reducing P_{net}) yields the largest gains, whereas thermal tuning has limited impact at room temperature because throttling is not activated in the tested setting.

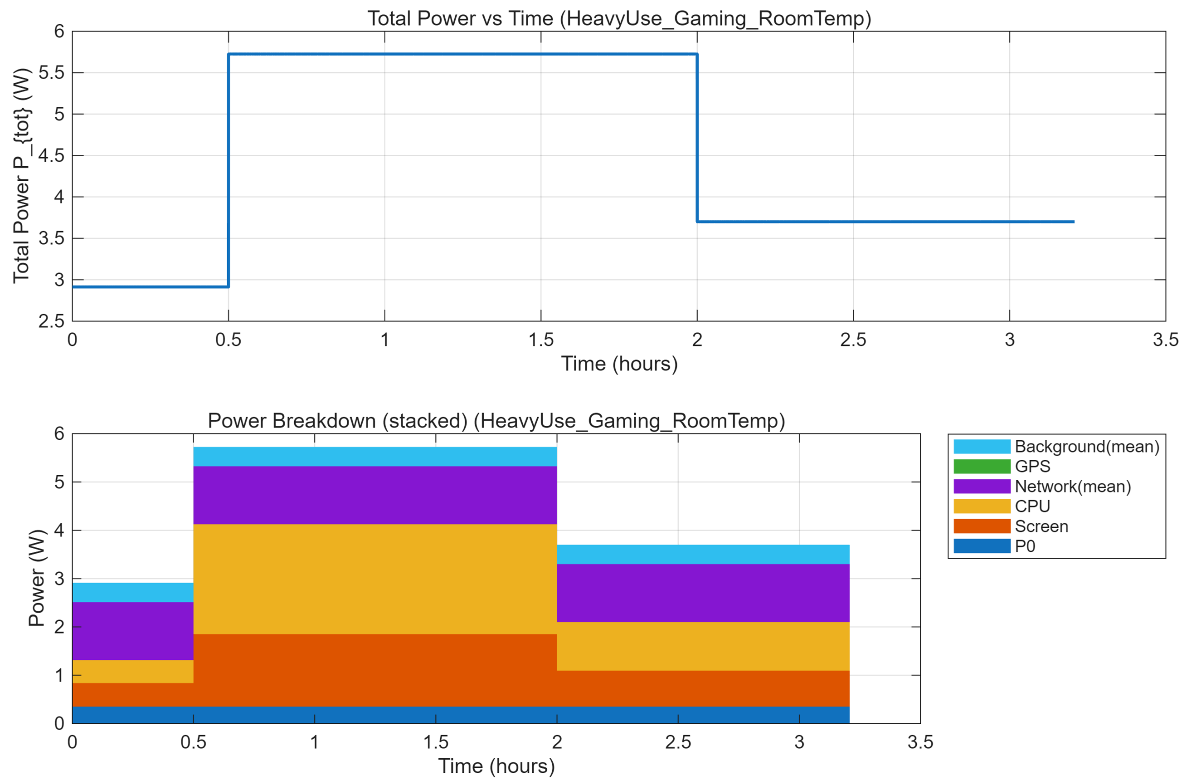

Figure 6: Total power and module breakdown for `HeavyUse_Gaming_RoomTemp`.

CPU and network dominate incremental demand in gaming, aligning with sensitivity results that rank P_{net} and CPU scaling among the most influential usage-driven parameters.

9 Sensitivity Analysis

9.1 Method

To quantify which parameters most influence predicted lifetime, we compute a normalized one-at-a-time sensitivity index:

$$S_\theta = \left| \frac{\Delta T_{\text{empty}} / T_{\text{empty}}}{\Delta \theta / \theta} \right|. \tag{13}$$

We apply $\pm 10\%$ perturbations around baseline values. This metric is dimensionless and comparable across parameters.

9.2 Findings and interpretation

Figure 7 shows sensitivities for the gaming scenario. The dominant driver is SOH, which enters linearly in Q_{eff} (Eq. (8)); thus a 10% change in health produces an approximately proportional change in usable charge, translating into a large change in T_{empty}. The next tier includes P_{net} and display scaling, which change mean power and directly change $\mathrm{d}SOC/\mathrm{d}t$ through Eq. (11). Thermal parameters are negligible in room-temperature cases because $T(t)$ never approaches the throttling threshold, making the thermal feedback weak.

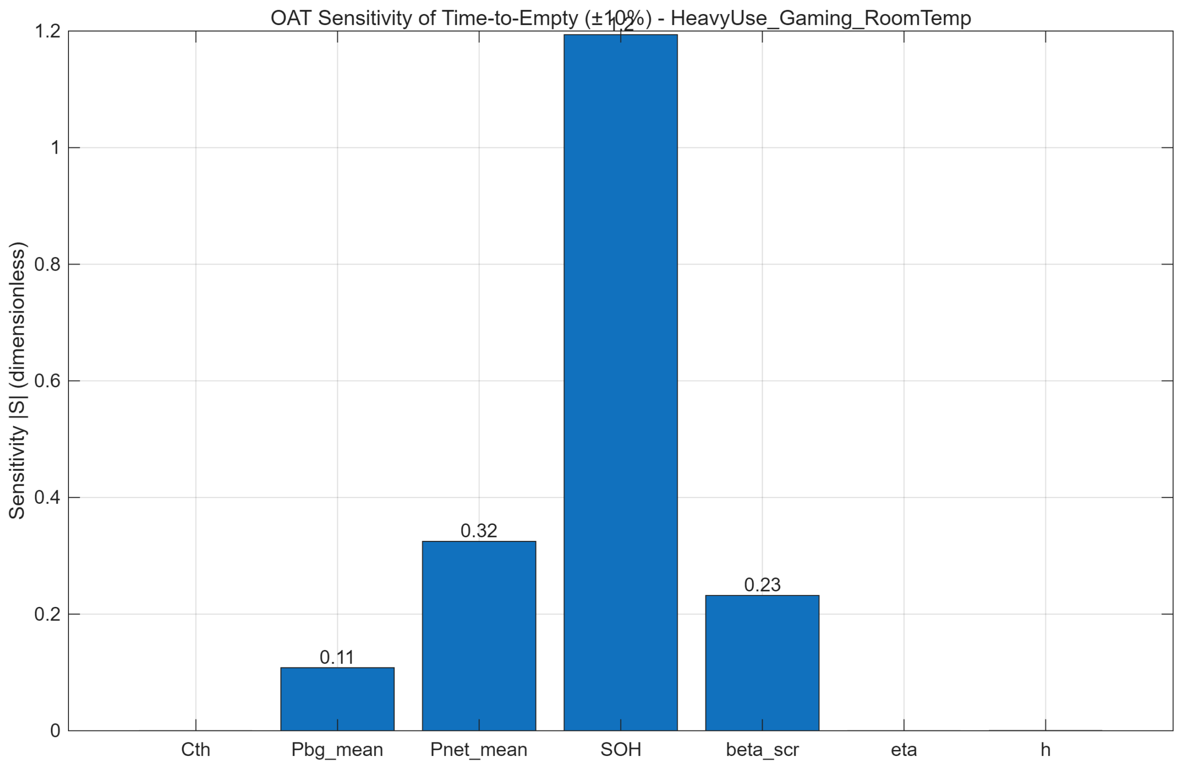

Figure 7: Sensitivity of T_{empty} to key parameters in the gaming scenario.

SOH dominates; network and display parameters follow. Thermal parameters are negligible under room-temperature conditions because temperature remains far from throttling thresholds.

Table 6: Top sensitivities for `HeavyUse_Gaming_RoomTemp` (OAT, ±10%).

Parameter θ	Sensitivity S_θ	Mechanism
SOH	1.194	scales usable charge via Q_{eff}
P_{net}	0.325	changes mean power in P_{tot}
β_{scr}	0.232	changes screen scaling
P_{bg}	0.108	persistent background drain
h	2.84×10^{-4}	weak at room temperature
C_{th}	9.0×10^{-5}	weak at room temperature
η	3.1×10^{-5}	weak at room temperature

10 Uncertainty Quantification (Monte Carlo)

10.1 Motivation and setup

Real battery drain is noisy because background and network loads fluctuate. To reflect this, we treat P_{bg} and P_{net} as random variables around their nominal values and repeatedly simulate the ODE system. Each run yields T_{empty}; the distribution quantifies predictive uncertainty.

10.2 Distribution and implications

Figure 8 shows the gaming time-to-empty distribution. The 95% interval $[2.762, 3.680]$ h spans nearly one hour, demonstrating that even with fixed "scenario labels," variability can shift battery life by tens of minutes. Therefore, user-facing forecasting should present an interval rather than a single point estimate.

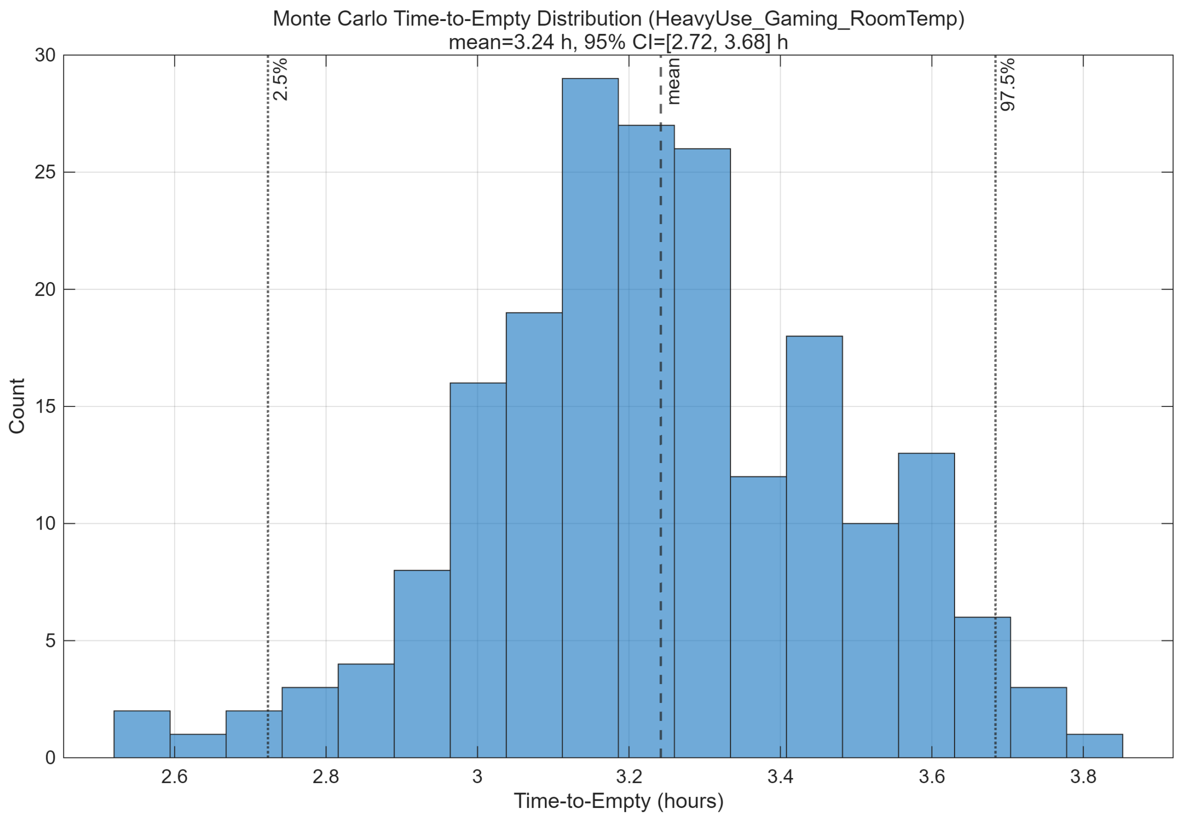

Figure 8: Monte Carlo distribution of T_{empty} for gaming. Mean = 3.242 h and 95% interval [2.762, 3.680] h.

Stochastic background/network loads produce substantial variability; reporting an uncertainty interval better reflects real usage.

11 What-if Analysis: Translating the model into actionable levers

A key advantage of an interpretable model is that it enables controlled what-if experiments. We summarize the most relevant levers and their expected magnitudes based on the sensitivity ranking.

11.1 Brightness and network interventions

Reducing brightness affects $P_{\text{scr}}(t)$ (Eq. (2)), while improved network conditions reduce P_{net} in Eq. (1). Table 7 reports qualitative impacts consistent with sensitivity ordering.

11.2 Cold mitigation

In cold navigation, the key lever is temperature through $f_T(T)$ (Eq. (9)). Keeping the phone warmer increases $T(t)$, thus increasing usable charge and extending time-to-empty. This differs from gaming, where thermal management is secondary and reducing mean power is primary.

Table 7: Illustrative what-if impacts (qualitative magnitudes guided by sensitivity ranking).

Intervention	Primary affected term(s)	Expected impact on T_{empty}
Reduce brightness by 20%	$\beta_{\text{scr}},\ b(t)$	moderate increase
Reduce network overhead by 20%	P_{net}	moderate increase
Reduce background drain by 20%	P_{bg}	small-to-moderate increase
Improve SOH by 10%	SOH	large increase

12 Recommendations

Based on mechanism separation, sensitivity ranking, and uncertainty analysis, we recommend:

- **Power-dominant cases (gaming/streaming):** reduce sustained CPU load and brightness; avoid weak-signal environments; close high-drain background processes. These act directly on $P_{\text{tot}}(t)$ in Eq. (1).
- **Capacity-dominant cases (cold navigation):** keep the phone warm to increase $f_T(T)$ in Eq. (9); pre-warm before outdoor navigation; reduce exposure to cold surfaces.
- **Prediction reporting:** present time-to-empty with an uncertainty band derived from Monte Carlo, especially when background/network variability is high.

13 Computational Complexity

Let N be the number of ODE solver evaluations per simulation. Each evaluation computes a constant number of algebraic operations, so each run costs $O(N)$. Sensitivity analysis over K parameters costs $O(KN)$, and Monte Carlo with M trials costs $O(MN)$. Therefore:

$$O\big((1 + K + M)N\big). \tag{14}$$

14 Strengths and Weaknesses

Strengths (4)

1. **Meets the continuous-time requirement:** explicit ODEs for $SOC(t)$ and $T(t)$ with event-stopping for T_{empty}.
2. **Interpretable attribution:** additive module structure clarifies which components dominate drain.
3. **Extensible and modular:** new sensors/apps enter through $P_{\text{tot}}(t)$ without rewriting the ODE core.
4. **Complete evaluation:** sensitivity, uncertainty (Monte Carlo), and computational complexity are included.

Weaknesses (2)

1. **Lumped thermal state:** a single temperature cannot capture spatial hot spots or multi-layer thermal gradients.
2. **Calibration dependency:** for high absolute accuracy on a specific phone, coefficients should be calibrated to device telemetry; here we emphasize mechanism-level realism and comparative insights.

15 Discussion: A mechanism-based view of battery life

A central insight from our results is that similar observed battery lifetimes can arise from different constraints. In a **power-dominant** regime, the key determinant is $\overline{P}_{\text{tot}}$, so reducing sustained load yields proportional improvements. In a **capacity-dominant** regime, the key determinant is $Q_{\text{eff}}(t)$, which can shrink due to cold temperature (via f_T) or aging (via SOH). These regimes require different interventions, and the model's modular structure provides both prediction and diagnosis.

Sensitivity analysis reinforces this: SOH dominates because it scales usable charge directly, while radios and display are the most actionable usage-dependent drivers. Finally, uncertainty analysis shows that variability is not negligible; practical prediction should include confidence intervals. Together, the model provides a contest-appropriate framework: mechanistic, interpretable, and quantitatively actionable.

16 References

References

[1] D. Bernardi, E. Pawlikowski, and J. Newman, "A General Energy Balance for Battery Systems," *Journal of the Electrochemical Society*, vol. 132, no. 1, pp. 5–12, 1985.

[2] G. L. Plett, "Extended Kalman filtering for battery management systems of LiPB-based HEV battery packs: Part 1. Background," *Journal of Power Sources*, vol. 134, no. 2, pp. 252–261, 2004.

[3] X. Hu, S. Li, and H. Peng, "A comparative study of equivalent circuit models for Li-ion batteries," *Journal of Power Sources*, vol. 198, pp. 359–367, 2012.

[4] C. Forgez, D. Vinh Do, G. Friedrich, M. Morcrette, and C. Delacourt, "Thermal modeling of a cylindrical $LiFePO_4$/graphite lithium-ion battery," *Journal of Power Sources*, vol. 195, no. 9, pp. 2961–2968, 2010.

[5] T. M. Bandhauer, S. Garimella, and T. F. Fuller, "A Critical Review of Thermal Issues in Lithium-Ion Batteries," *Journal of the Electrochemical Society*, vol. 158, no. 3, pp. R1–R25, 2011.

[6] F. P. Incropera and D. P. DeWitt, *Fundamentals of Heat and Mass Transfer*, 7th ed., Wiley, 2011.

[7] J. Vetter, P. Novák, M. R. Wagner, C. Veit, K.-C. Möller, J. O. Besenhard, M. Winter, M. Wohlfahrt-Mehrens, C. Vogler, and A. Hammouche, "Ageing mechanisms in lithium-ion batteries," *Journal of Power Sources*, vol. 147, no. 1–2, pp. 269–281, 2005.

AI Use Report

Our team made limited use of generative AI tools solely for **language and formatting assistance**. Specifically, AI was used to:

- **Language refinement:** grammar checking, reducing redundancy, and improving clarity and coherence of written text;
- **Formatting support:** verifying LaTeX consistency (figure/table captions and placement, numbering and cross-references, table of contents, and page header/page numbering);
- **Code organization:** providing debugging suggestions and style improvements for team-written MATLAB scripts (e.g., variable naming, plotting consistency, preventing redundant figures).

All **modeling choices** (assumptions, equations, parameter settings), **scenario design**, **computations**, **experiments**, and **interpretation of results and conclusions** were performed and finalized by the team. AI tools were **not** used to replace the team's reasoning for model development or decision-making.